Biochimica et Biophysica Acta 1848 (2015) 527–531

Contents lists available at ScienceDirect

Biochimica et Biophysica Acta

journal homepage: www.elsevier.com/locate/bbamem

# Membrane sorting via the extracellular matrix

Sina Sadeghi *, Richard L.C. Vink

*Institute of Theoretical Physics, Georg-August-Universität Göttingen, Friedrich-Hund-Platz 1, D-37077 Göttingen, Germany*

ARTICLE INFO

*Article history:*
Received 27 June 2014
Received in revised form 6 October 2014
Accepted 21 October 2014
Available online 8 November 2014

*Keywords:*
Bilayer membrane structure
Membrane curvature
Lipid raft
Monte Carlo simulation
Statistical physics

ABSTRACT

We consider the coupling between a membrane and the extracellular matrix. Computer simulations demonstrate that the latter coupling is able to sort lipids. It is assumed that membranes are elastic manifolds, and that this manifold is disrupted by the extracellular matrix. For a solid-supported membrane with an actin network on top, regions of positive curvature are induced below the actin fibers. A similar mechanism is conceivable by assuming that the proteins which connect the cytoskeleton to the membrane induce local membrane curvature. The regions of non-zero curvature exist irrespective of any phase transition the lipids themselves may undergo. For lipids that prefer certain curvature, the extracellular matrix thus provides a spatial template for the resulting lateral domain structure of the membrane.



## 1. Introduction

Ever since the lipid raft hypothesis has been established [1], the lateral organization of membranes has been intensely studied. Much has been learned from model membranes, in which the number of lipid species is strongly reduced compared to their biological counterparts, enabling detailed and systematic investigations [2,3]. The hope is that a good understanding of the model system will also provide valuable insight into biological membranes.

Investigations of model membranes have established one fact beyond any doubt, namely the occurrence of phase transitions in these systems. For example, ternary membrane mixtures containing saturated lipids, unsaturated lipids, and cholesterol, demix into two fluid phases upon lowering the temperature [4]. Furthermore, in single component membranes, there exists the main transition, between a phase where the lipid tails are ordered, and one where the tails are disordered [5,6]. Consequently, it is tempting to assume that phase transitions play a key role in biological membranes as well [7,8]. Of course, a minimal condition for this hypothesis is that all biological membranes operate at conditions that are close to phase transitions. Given the enormous diversity in membrane compositions between cells, different "body" temperatures between species, coupling of the membrane to active processes in the cell cortex [9], an intriguing mechanism must have evolved to keep the membrane "tuned" to the vicinity of a phase transition. While such a mechanism may well exist, its details remain elusive to this day.

The purpose of this paper is to highlight that phase transitions are not the only means to bring about lateral organization in biological membranes. In our view, a key difference between biological and model membranes is the presence of an extracellular matrix in the former: A biological membrane is not free, but instead intricately connected to its environment, for example to the cytoskeleton network. As we will show for a very simple model, the mere connection to the environment is already sufficient to induce lateral organization. Our model is inspired by a recent experiment of a (model) membrane "sandwiched" between a substrate and an actin network [10]. This experiment revealed a lateral domain structure in the membrane that was strongly correlated to the actin fibers. We will show here how the interplay between the substrate, the actin network, and the membrane elastic properties already provides a "template" for this structure, i.e. completely independent of any phase transition the lipids may exhibit. Next, we consider how such a mechanism could manifest itself in situations where a substrate is absent, but where the proteins that connect the cytoskeleton to the membrane induce local membrane curvature. Our proposed mechanisms are in line with recent studies that also indicate the importance of the cytoskeleton in bringing about lateral organization, such as the formation of protein–lipid complexes [11], and GPI-anchored protein clusters [12]. In addition, the coupling to the cytoskeleton induces spatial confinement, which affects the spectrum of membrane height fluctuations [13–15], as well as protein diffusion [16,17].

## 2. Model and method

Our membrane model is defined on a two-dimensional (2D) $L \times L$ periodic square lattice. To describe the out-of-plane height deformations, each lattice site $i$ is given a real number $h_i$ to denote the local membrane height (Monge representation). We consider a membrane that strongly interacts with its environment. This interaction, for

* Corresponding author. Tel.: +49 551 39 22067; fax: +49 551 39 9631.
*E-mail address:* sadeghi@theorie.physik.uni-goettingen.de (S. Sadeghi).

http://dx.doi.org/10.1016/j.bbamem.2014.10.035

instance with the solid substrate or the cytoskeleton network, will typically constrain the membrane height fluctuations. In general, the free energy of the system is given by

$$\mathcal{H} = \frac{\kappa a^2}{2}\sum_i \left(\nabla^2 h_i\right)^2 + \mathcal{H}_{\text{env}}, \tag{1}$$

where $a$ is the lattice spacing, and the sum is over all lattice sites. The first term in Eq. (1) is the elastic energy of the membrane, given in lowest order of the Helfrich expansion with $\kappa$ being the bending modulus [18]. On the lattice, the Laplacian is expressed using the standard finite-difference expression [19]. The second term $\mathcal{H}_{\text{env}}$ describes the membrane–environment interaction, and needs to be defined explicitly for the case of interest.

We perform Monte Carlo (MC) to simulate Eq. (1). The MC move is to update the height of a randomly selected lattice site. To this end, we propose a new height for the chosen site and accept it with the Metropolis probability, $P_{\text{acc}} = \min[1, e^{-\beta\Delta\mathcal{H}}]$, where $\beta = 1/k_{\text{B}}T$ with $k_{\text{B}}$ as the Boltzmann constant, $T$ as the temperature, and $\Delta\mathcal{H}$ as the free energy difference computed according to Eq. (1). For a free energy $\mathcal{H}$ that is quadratic in the height, $\sim \sum_i (A_i h_i^2 + B_i h_i)$, one can optimally propose the new height to the chosen site $i$ from a Gaussian distribution with mean $-B_i/2A_i$ and variance $k_{\text{B}}T/2A_i$ [20], which is how the present simulations are performed.

## 3. Results

### 3.1. Membrane "sandwiched" between a solid substrate and an actin network

We first consider a solid-supported membrane bound to an actin network, which resembles the situation addressed experimentally in Ref. [10]. In this case, the interaction potential in Eq. (1) is given by

$$\mathcal{H}_{\text{env}} = \mathcal{H}_{\text{sub}} + \mathcal{H}_{\text{act}}, \tag{2}$$

where the first term describes the interaction of the membrane with the solid support, and the second term describes the influence of the actin network.

Solid-supported membranes are separated from the substrate by an ultra-thin hydration layer typically 1 nm thick. Consequently, the membrane–substrate interaction is a strong one [21–24]. It can be expressed as a superposition of repulsive hydration (steric) and attractive van der Waals forces [25]. This typically results in a membrane–substrate interaction featuring a minimum some distance above the support. We expand up to quadratic order around the minimum, leading to

$$\mathcal{H}_{\text{sub}} = \frac{\alpha a^2}{2}\sum_i h_i^2, \tag{3}$$

where $\alpha$ is the strength of the harmonic potential [26,27]. For simplicity, the minimum of the harmonic potential is set to $h = 0$, which we take as the reference from which the membrane height variables $h_i$ are measured. We emphasize that by using a harmonic potential, the free energy Eq. (1) remains quadratic in $h_i$ and so we can use the Gaussian distribution method of Ref. [20] to optimally propose new height variables during the MC simulations.

Next, we describe the effect of the actin term $\mathcal{H}_{\text{act}}$. In the experiment of Ref. [10], an actin network is deposited on top of the supported membrane, i.e. the membrane is "sandwiched" between the substrate and the actin network. In experiments [10,28], actin is bound to the membrane via cross-linker molecules, such as streptavidin, referred to as *pinning sites* in what follows. The pinning sites are immobilized obstacles randomly distributed along the actin fibers. In line with previous simulations [10,28,29], we represent the actin network by a Voronoi diagram obtained from a set of random points. The thickness of the actin fibers is one lattice site, the typical compartment size is chosen to be ~ 100 nm. The resulting Voronoi diagram is then superimposed on the lattice of height variables. Next, we place the pinning sites, at randomly selected points along the edges of the Voronoi diagram. Once put in place, the pinning sites remain fixed, i.e. they cannot diffuse along the actin fibers. We assume that the effect of a pinning site is to locally push the membrane down, i.e. away from the reference height $h = 0$ toward negative values. We incorporate this effect into our simulations by fixing the height variable at each pinning site to a negative value $h_{\text{P}} < 0$ (for simplicity, the same value $h_{\text{P}}$ is used for all the pinning sites). During the simulations, MC moves are thus *not* applied to pinning sites. Since Eq. (3) is a quadratic expansion, our analysis is restricted to small values of $h_{\text{P}}$. An extreme upper bound is the thickness of the hydration layer ~10 Å, which is the maximum distance the membrane can be pushed down, and where Eq. (3) certainly breaks down. For this reason, in the analysis to be presented, we restrict $h_{\text{P}}$ to several Å at most.

We simulate a system of size $L = 400$ with lattice spacing $a = 2$ nm. For the presented results, we use a typical value $\beta\kappa = 70$ for the bending rigidity [27,30]. At room temperature, $T = 300$ K, this corresponds to $\kappa = 2.9 \times 10^{-19}$ Nm, which is close to the value used in Ref. [10]. Fig. 1 shows a snapshot of the membrane, color-coded according to the thermally averaged height (left) and curvature (right). In both cases 25% of the actin network is covered by pinning sites. Results are presented for two values of the strength of the harmonic potential, $\beta\alpha a^4 = 2$ (a) and $\beta\alpha a^4 = 4$ (b). The reported values of $\alpha$ in literature cover quite a wide range [20,26,27]. Our results use values comparable to $k_{\text{B}}T$ [20]. The deviation from the reference height at the pinning sites is set as $h_{\text{P}} = -6$ Å. The simulations ran for $4 \times 10^6$ sweeps, after having been equilibrated for $4 \times 10^5$ sweeps (each sweep is $L^2$ attempted MC moves).

As can be seen from height and curvature profiles, the actin pattern is clearly "pressed" onto the membrane. In particular, in the curvature snapshots, one can see that along the actin fibers an on-average positive curvature has been induced. This effect persists even at low fractions of pinning sites. To quantify this, we measured the cross correlation between the curvature snapshot $\mathbf{c}$ and the actin network $\mathbf{a}$ using the Pearson correlation coefficient (PCC). The advantage of using this quantity is that it can also be measured in experiments via fluorescence spectroscopy [10]. The PCC is defined as

$$\text{PCC} = \frac{\sum_i (\mathbf{c}_i - \bar{\mathbf{c}})(\mathbf{a}_i - \bar{\mathbf{a}})}{\sqrt{\sum_i (\mathbf{c}_i - \bar{\mathbf{c}})^2}\sqrt{\sum_i (\mathbf{a}_i - \bar{\mathbf{a}})^2}}, \tag{4}$$

where $\bar{\mathbf{c}}$ and $\bar{\mathbf{a}}$ are the mean "pixel" values of the curvature and actin images, and the sum over all lattice sites (for the actin image, $\mathbf{a}_i$ is zero everywhere except at sites that intersect with an edge of the Voronoi network, for which $\mathbf{a}_i = 1$). A positive (negative) value of PCC means that the curvature is positive (negative) on average underneath the actin fibers, while a value of zero means that there is no correlation.

Fig. 2(a) shows how PCC varies with the pinning fraction, using $h_{\text{P}} = -6$ Å. The PCC initially increases linearly from zero with the pinning fraction. In the linear regime, the pinning sites are isolated from each other. Each pinning site thus contributes to the PCC by the same amount, which explains the linear increase. At larger pinning fractions, the pinning sites are no longer isolated, i.e. their "regions of influence" begin to overlap, which explains the downward curvature in the data. The effect of the pinning height $h_{\text{P}}$ is shown in Fig. 2(b) for a pinning fraction of 40%: By pushing the membrane further down, PCC increases.

For a solid-supported membrane with an actin network "on-top", these results suggest a mechanism for lateral domain formation in membranes that does not require any phase separation between lipids. The pinning sites along the actin fibers locally push the membrane down, leading to non-zero average curvature below the fibers. Consider now a lipid mixture, with one of the lipid species preferring regions of, say, positive curvature (the coupling between membrane composition

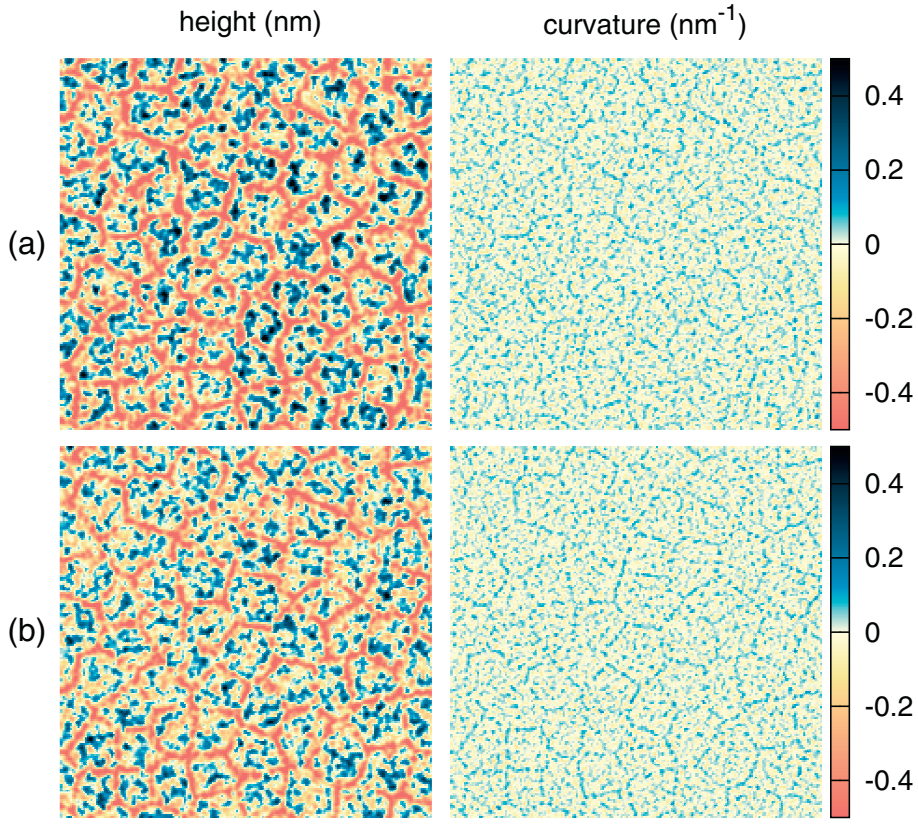


**Fig. 1.** Typical snapshots of the thermally averaged height and curvature profiles of the solid-supported membrane bound to an actin network, in units of nm and nm$^{-1}$, respectively. The strength of harmonic potential is given $\beta\alpha a^4 = 2$ and 4 for (a) and (b) respectively. In both cases, the pinning fraction is 25% of entire actin network and the pinning deviation height $h_P = -6$ Å.

and curvature is an established fact [30–35]). In the upper membrane leaflet, these lipids would then preferentially collect underneath the actin fibers, since there the curvature has the correct sign. In contrast, in the lower leaflet where the curvature sign is reversed, these lipids would be repelled from the fibers. Hence, a domain pattern (in this case anti-correlated between the two leaflets) can be induced purely by the coupling between the local membrane curvature and the curvature preferred by a single lipid species. This pattern is independent of the energetic interaction between the lipids, i.e. it does not require the lipid mixture to be close to any demixing phase transition. We emphasize that the formation of anti-correlated domains requires the composition to be the same in both leaflets [30]. In case this condition is not met, the coupling between the leaflets is more complex, and also correlated domains are possible [31].

### 3.2. Pinning sites that induce local membrane curvature

We now argue that a similar mechanism as proposed above for a solid-supported membrane could persist in the absence of a substrate

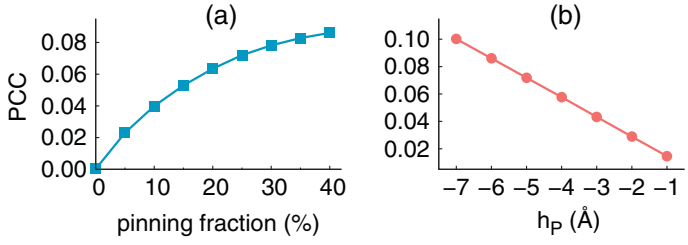


**Fig. 2.** (a) The variation of the Pearson correlation coefficient (PCC) with the pinning fraction for $h_P = -6$ Å. (b) PCC versus $h_P$ for pinning fraction of 40%. In both plots, the strength of the harmonic potential $\beta\alpha a^4 = 4$.

also. This mechanism is based on the observation that proteins associated with actin can be curved, owing to their geometry (examples include IMD [36] and IRSp53 [37] proteins). In our model, this effect can be incorporated by assuming that the pinning sites induce a non-zero local membrane curvature, say, of value $C_p$. Within this framework, the Helfrich bending energy reads as

$$\mathcal{H}_{\text{bend}} = \frac{\kappa a^2}{2}\sum_i \left(\nabla^2 h_i - C_p\delta_i\right)^2, \tag{5}$$

where $\delta_i = 1$ in case lattice site $i$ is a pinning site, and zero otherwise. Expanding the square (and dropping an irrelevant constant), one obtains Eq. (1) with

$$\mathcal{H}_{\text{env}} = -\kappa C_p a^2 \sum_i \left(\nabla^2 h_i\right)\delta_i, \tag{6}$$

which describes the effect of the pinning sites [35]. In the previous model for the solid-supported membrane, the pinning sites were assumed to locally push the membrane down. In the present model, they are assumed to induce local membrane curvature. The model, as before, is readily simulated using our MC procedure. We emphasize that since the free energy remains quadratic, one can still use the Gaussian distribution to optimally propose new height values [20]. In contrast to the solid-supported membrane, the MC moves in the present model are applied to all lattice sites.

Fig. 3 shows typical snapshots of the thermally averaged curvature values obtained for the model of Eq. (5). The curvature radius of the pinning sites is set as $C_p^{-1} = 2$ nm in both cases [38,39]. The snapshots correspond to pinning fraction of 25% and 40% of the entire actin network, for (a) and (b), respectively. The correlation between the positively curved regions and the actin fibers increases as the pinning fraction increases. This is manifested by the PCC, shown in Fig. 4(a). Note that the

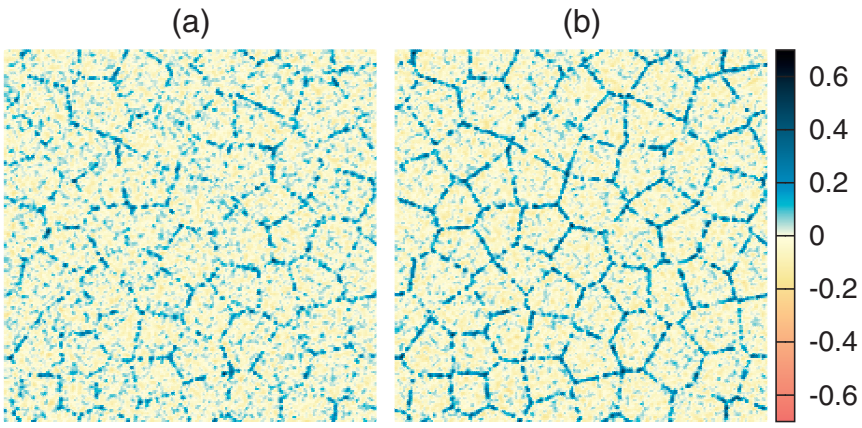


**Fig. 3.** Typical snapshots of the thermally averaged curvature profile for the membrane model of Eq. (5), where the pinning sites induce local membrane curvature. The pinning fractions are 25% (a) and 40% (b) of the entire actin network. The curvature radius of the pinning sites $C_P^{-1} = 2$ nm in both cases.

PCC values significantly exceed those of Fig. 2(a). As might be expected, pinning sites that directly impose local membrane curvature are more efficient at imprinting a curvature pattern than pinning sites that couple to the membrane height. We also measured the PCC as a function of the curvature radius of the pinning sites $C_P^{-1}$, see Fig. 4(b). As can be seen, by increasing the curvature radius of the pinning sites, the PCC decreases. This is to be expected since the limit $C_P \to 0$ describes pinning sites that prefer the membrane to be locally flat.

Hence, also in this case, a lateral domain pattern may already be "imprinted" via the coupling of the membrane to the actin network. The preferred local membrane curvature "stamped" onto the membrane sheet by the pinning sites induces regions that are favorable for lipids of matching spontaneous curvature. As in the case of the solid-supported membrane, this provides a mechanism of sorting lipids via curvature, and which does not require the lipids to be near a demixing transition.

## 4. Discussion

In this paper, we have proposed an alternative mechanism able to sort lipids in membranes. The mechanism is based on the fact that membranes are elastic manifolds, and that this manifold is disrupted by the presence of the extracellular matrix. In the case of a solid-supported membrane with an actin network "on-top", MC simulations reveal that regions of positive curvature are induced underneath the actin fibers. A similar mechanism is conceivable by assuming that the proteins which connect the cytoskeleton to the membrane, induce local non-zero curvature. The regions of non-zero curvature exist irrespective of any phase transition the lipids themselves may undergo. Hence, even for a lipid mixture at high temperature, i.e. above the temperature of phase separation, lipid sorting can still take place provided that the lipid species have different affinities to curvature. In the presented models, lipids that prefer positive curvature would collect underneath the actin strands.

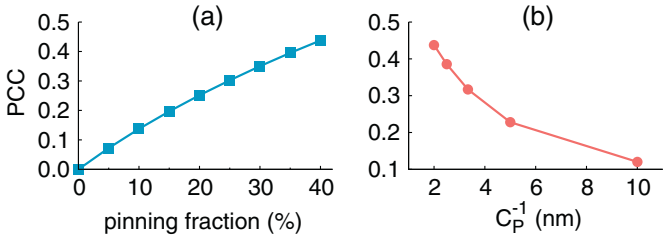


**Fig. 4.** Pearson correlation coefficient (PCC) for the membrane model of Eq. (5). (a) PCC vs. pinning fraction for $C_P^{-1} = 2$ nm. (b) PCC vs. the curvature radius of the pinning sites at pinning fraction of 40%.

In realistic situations, there will be an interplay between the proposed curvature mechanism and other mechanisms. For example, it could be that the pinning sites also energetically attract certain lipid species, for instance via electrostatic interactions. The species that is attracted energetically need not be the same as the species preferred by curvature. In this case, the resulting lipid domain structure is determined by the relative strength of each source of attraction. Recent experiments suggest that such an interplay indeed occurs [10]. In this experiment, a ternary membrane mixture containing saturated/unsaturated lipids and cholesterol was used. The membrane was connected to an actin network via pinning sites, and the energetic attraction of the pinning sites could be controlled. For pinning sites that weakly attract saturated lipids, nevertheless a small excess of unsaturated lipids along the actin fibers was observed. This result shows that other mechanisms, beyond the energetic attraction between lipids and pinning sites, are at work that determine the lateral domain structure. Computer simulations in which the energetic and curvature attractions are both included are indeed able to reproduce the experimental results [10].

In view of raft formation, the coupling between membrane lipid composition and local curvature is currently attracting much attention [30,31,40]. It has been shown that such a coupling is able to induce composition fluctuations on a length scale of 10–100 nm, which is compatible with the size of rafts. In combination with the coupling to the extracellular matrix presented in this paper, this mechanism can be extended, providing cells with a means to control the spatial location where rafts are formed (for instance underneath actin strands). A further interesting extension would be to include the role of active processes in the cell cortex, such that the positions of the pinning sites become time-dependent. In this situation, there can even be a feedback between the local membrane curvature due to curved proteins that are associated with the actin, and the recruitment of actin [41,42].

## Acknowledgments

This work was supported by the Deutsche Forschungsgemeinschaft within the collaborative research center, grant no. SFB-937 (Collective Behavior of Soft and Biological Matter, project A6), and the Emmy Noether Program (VI 483).

## References

[1] Simons, Ikonen, Functional rafts in cell membranes, Nature 387 (1997) 569.
[2] Simons, Vaz, Model systems, lipid rafts, and cell membranes, Annu. Rev. Biophys. Biomol. Struct. 33 (2004) 269.
[3] Dietrich, Bagatolli, Volovyk, Thompson, Levi, Jacobson, Gratton, Lipid rafts reconstituted in model membranes, Biophys. J. 80 (2001) 1417.
[4] Veatch, Keller, Organization in lipid membranes containing cholesterol, Phys. Rev. Lett. 89 (2002) 268101.

[5] Nagle, Theory of the main lipid bilayer phase transition, Annu. Rev. Phys. Chem. 31 (1980) 157.
[6] Charrier, Thibaudau, Main phase transitions in supported lipid single-bilayer, Biophys. J. 89 (2005) 1094.
[7] Levental, Byfield, Chowdhury, Gai, Baumgart, Janmey, Cholesterol-dependent phase separation in cell-derived giant plasma-membrane vesicles, Biochem. J. 424 (2009) 163.
[8] Veatch, Keller, Seeing spots: complex phase behavior in simple membranes, Biochim. Biophys. Acta 1746 (2005) 172.
[9] Mayor, Rao, Rafts: scale-dependent, active lipid organization at the cell surface, Traffic 5 (2004) 231.
[10] Honigmann, Sadeghi, Keller, Hell, Eggeling, Vink, A lipid bound actin meshwork organizes liquid phase separation in model membranes, eLife 3 (2014) e01671.
[11] Gómez-Llobregat, Buceta, Reigada, Interplay of cytoskeletal activity and lipid phase stability in dynamic protein recruitment and clustering, Sci. Rep. 3 (2013) 2608.
[12] Goswami, Gowrishankar, Bilgrami, Ghosh, Raghupathy, Chadda, Vishwakarma, Rao, Mayor, Nanoclusters of GPI-anchored proteins are formed by cortical actin-driven activity, Cell 135 (2008) 1085.
[13] Gov, Safran, Pinning of fluid membranes by periodic harmonic potentials, Phys. Rev. E. 69 (2004) 011101.
[14] Farago, Membrane fluctuations near a plane rigid surface, Phys. Rev. E. 78 (2008) 051919.
[15] Farago, Statistical thermodynamics of adhesion points in supported membranes, Adv. Planar Lipid Bilayers Liposomes 14 (2011) 129.
[16] Kusumi, Nakada, Ritchie, Murase, Suzuki, Murakoshi, Kasai, Kondo, Fujiwara, Paradigm shift of the plasma membrane concept from the two-dimensional continuum fluid to the partitioned fluid: high-speed single-molecule tracking of membrane molecules, Annu. Rev. Biophys. Biomol. Struct. 34 (2005) 351.
[17] Lin, Brown, Dynamic simulations of membranes with cytoskeletal interactions, Phys. Rev. E. 72 (2005) 011910.
[18] Helfrich, Elastic properties of lipid bilayers: theory and possible experiments, Z. Naturforsch. 28c (1973) 693.
[19] Weikl, Andelman, Komura, Lipowsky, Adhesion of membranes with competing specific and generic interactions, Eur. Phys. J. E: Soft Matter Biol. Phys. 8 (2002) 59.
[20] Speck, Vink, Random pinning limits the size of membrane adhesion domains, Phys. Rev. E. 86 (2012) 031923.
[21] Sackmann, Supported membranes: scientific and practical applications, Science 271 (1996) 43.
[22] Salditt, Thermal fluctuations and stability of solid-supported lipid membranes, J. Phys. Condens. Matter 17 (2005) R287.
[23] Lipowsky, Generic Interactions of Flexible Membraneschap. Ch. 11, Elsevier, 1995. 521.
[24] Seifert, Configurations of fluid membranes and vesicles, Adv. Phys. 13 (1997).
[25] Rädler, Feder, Strey, Sackmann, Fluctuation analysis of tension-controlled undulation forces between giant vesicles and solid substrates, Phys. Rev. E. 51 (1995) 4526.
[26] Reister, Bihr, Seifert, Smith, Two intertwined facets of adherent membranes: membrane roughness and correlations between ligand–receptors bonds, New J. Phys. 13 (2011) 025003.
[27] Speck, Reister, Seifert, Specific adhesion of membranes: mapping to an effective bond lattice gas, Phys. Rev. E. 82 (2010) 021923.
[28] Machta, Papanikolaou, Sethna, Veatch, Minimal model of plasma membrane heterogeneity requires coupling cortical actin to criticality, Biophys. J. 100 (2011) 1668.
[29] Ehrig, Petrov, Schwille, Near-critical fluctuations and cytoskeleton-assisted phase separation lead to subdiffusion in cell membranes, Biophys. J. 100 (2011) 80.
[30] Schick, Membrane heterogeneity: manifestation of a curvature-induced microemulsion, Phys. Rev. E. 85 (2012) 031902.
[31] Shlomovitz, Schick, Model of a raft in both leaves of an asymmetric lipid bilayer, Biophys. J. 105 (2013) 1406.
[32] Parthasarathy, Yu, Groves, Curvature-modulated phase separation in lipid bilayer membranes, Langmuir 22 (2006) 5095.
[33] Parthasarathy, Groves, Curvature and spatial organization in biological membranes, Soft Matter 3 (2007) 24.
[34] Liu, Qi, Groves, Chakraborty, Phase segregation on different length scales in a model cell membrane system, J. Phys. Chem. B 109 (2005) 19960.
[35] Leibler, Andelman, Ordered and curved meso-structures in membranes and amphiphilic films, J. Phys. 48 (1987) 2013.
[36] Mattila, Pykalainen, Saarikangas, Paavilainen, Vihinen, Jokitalo, Lappalainen, Missing-in-metastasis and IRSp53 deform PI(4,5)P2-rich membranes by an inverse BAR domain-like mechanism, J. Cell Biol. 176 (2007) 953.
[37] Scita, Confalonieri, Lappalainen, Suetsugu, IRSp53: crossing the road of membrane and actin dynamics in the formation of membrane protrusions, Trends Cell Biol. 18 (2008) 52.
[38] Sorre, Callan-Jones, Manzi, Goud, Prost, Bassereau, Roux, Nature of curvature coupling of amphiphysin with membranes depends on its bound density, Proc. Natl. Acad. Sci. 109 (2012) 173.
[39] Zimmerberg, Kozlov, How proteins produce cellular membrane curvature, Nat. Rev. Mol. Cell Biol. 7 (2005) 9.
[40] Meinhardt, Vink, Schmid, Monolayer curvature stabilizes nanoscale raft domains in mixed lipid bilayers, Proc. Natl. Acad. Sci. 110 (2013) 4476.
[41] Gov, Gopinathan, Dynamics of membranes driven by actin polymerization, Biophys. J. 90 (2006) 454.
[42] Veksler, Gov, Phase transitions of the coupled membrane-cytoskeleton modify cellular shape, Biophys. J. 93 (2007) 3798.